Molecular and Cellular Neuroscience 119 (2022) 103705

Contents lists available at ScienceDirect

Molecular and Cellular Neuroscience

journal homepage: www.elsevier.com/locate/ymcne

Differential expression of the neuronal CB1 cannabinoid receptor in the hippocampus of male Ts65Dn Down syndrome mouse model

Nadia Di Franco [1], Guillaume Drutel [1], Valérie Roullot-Lacarrière, Francisca Julio-Kalajzic, Valérie Lalanne, Agnès Grel, Thierry Leste-Lasserre, Isabelle Matias, Astrid Cannich, Delphine Gonzales, Vincent Simon, Daniela Cota, Giovanni Marsicano, Pier Vincenzo Piazza [2], Monique Vallée [1], Jean-Michel Revest [*,1]

Univ. Bordeaux, INSERM, Neurocentre Magendie, U1215, F-33000 Bordeaux, France

ARTICLE INFO

Keywords:
Endocannabinoid system (ECS)
Cannabinoid type-1 receptor (CB1)
Down syndrome (DS)
Ts65Dn mouse
Hippocampus (HPC)

ABSTRACT

Down syndrome (DS) or Trisomy 21 is the most common genetic cause of mental retardation with severe learning and memory deficits. DS is due to the complete or partial triplication of human chromosome 21 (HSA21) triggering gene overexpression and protein synthesis alterations responsible for a plethora of mental and physical phenotypes. Among the diverse brain target systems that affect hippocampal-dependent learning and memory deficit impairments in DS, the upregulation of the endocannabinoid system (ECS), and notably the overexpression of the cannabinoid type-1 receptor (CB1), seems to play a major role. Combining various protein and gene expression targeted approaches using western blot, qRT-PCR and FISH techniques, we investigated the expression pattern of ECS components in the hippocampus (HPC) of male Ts65Dn mice. Among all the molecules that constitute the ECS, we found that the expression of the CB1 is altered in the HPC of Ts65Dn mice. CB1 distribution is differentially segregated between the dorsal and ventral part of the HPC and within the different cell populations that compose the HPC. CB1 expression is upregulated in GABAergic neurons of Ts65Dn mice whereas it is downregulated in glutamatergic neurons. These results highlight a complex regulation of the CB1 encoding gene (*Cnr1*) in Ts65Dn mice that could open new therapeutic solutions for this syndrome.

1. Introduction

Each year, Down syndrome (DS) or Trisomy 21, for which there is currently no pharmacological treatment, affects 1 in 650 newborns in the United States and 1 in 1000 in Europe (Caban-Holt et al., 2015). It is the most common genetic cause of mental retardation with severe learning and cognitive deficits (CD) (Gardiner et al., 2010). DS is characterized by a plethora of physical phenotypes that impact many body systems (Dierssen, 2012) as a result of aberrant gene regulation. DS is caused by the presence of an extra full or partial chromosome 21 (HSA21), which triggers gene overexpression (Lana-Elola et al., 2011) and protein synthesis alterations (Antonarakis, 2017) contributing to the pathological phenotypes of DS (Ahmed et al., 2012). Although physical rehabilitation and surgical procedures at birth have helped patients to develop normally (Vis et al., 2009), CD prohibit them from leading a normal life (Gardiner, 2015) reflecting the need to identify new brain

Abbreviations: AA, arachidonic acid; ABHD12, α,β-hydrolase-12; AEA, anandamide; AD, Alzheimer-like disease; *CA1*, *2* or *3*, Cornus Ammonis 1, 2 or 3; CB1, cannabinoid type-1 receptor; CB2, cannabinoid type-2 receptor; CD, cognitive deficit; *Cnr1*, CB1 encoding gene; *Cnr2*, CB2 encoding gene; D-FISH, double fluorescent *in situ* hybridization; DAGL, diacylglycerol lipase; *DG*, Dentate Gyrus; dHPC, dorsal hippocampus; DS, Down syndrome; eCBs, endocannabinoids; ECS, endocannabinoid system; ETA, ethanolamine; FAAH, fatty acid amide hydrolase; GAD, glutamic acid decarboxylase 65 kDa and 67 kDa; HSA21, human chromosome 21; *LMol*, lacunosum moleculare strata; MAGL, monoacylglycerol lipase; NAPE, N-acyl phosphatidylethanolamine; NAPE-PLD, N-acyl phosphatidylethanolamine phospholipase D; PFC, prefrontal cortex; PIP2, phosphatidylinositol 4,5-bisphosphate; PLC, phospholipase C; *Po*, polymorph dentate gyrus; *Py*, pyramidal layers; *SLu*, stratum lucidum; vHPC, ventral hippocampus; 2-AG, 2-arachidonoylglycerol.

* Corresponding author at: Univ. Bordeaux, INSERM, Neurocentre Magendie, U1215, F-33000 Bordeaux, France.
E-mail address: jean-michel.revest@inserm.fr (J.-M. Revest).
[1] These authors contributed equally to this work.
[2] Current address: Aelis Farma, 33077 Bordeaux, France.

https://doi.org/10.1016/j.mcn.2022.103705
Received 13 December 2021; Received in revised form 27 January 2022; Accepted 8 February 2022
Available online 11 February 2022

molecular targets for CD in DS (Sturgeon et al., 2012).

To this aim, we used the DS mouse model Ts65Dn (Davisson et al., 1990). Among the different models (Herault et al., 2017), Ts65Dn mice have the best face validity as they recapitulate the majority of phenotypes observed in DS, including learning and memory impairments (Reeves et al., 1995; Escorihuela et al., 1998; Martínez-Cué et al., 2002). The CD occurring both in DS subjects and Ts65Dn mice are mainly due to neuroanatomical and functional alterations in brain areas related to cognition, in particular the hippocampus (HPC) (Insausti et al., 1998; Aylward et al., 1999; Teipel et al., 2003; Kurt et al., 2004; Lorenzi and Reeves, 2006).

Among the diverse brain target systems that affect hippocampal-dependent CD, the endocannabinoid system (ECS) has been shown to play a major role (Marsicano and Lafenêtre, 2009; Puighermanal et al., 2012). The ECS is a biological signaling system that encompasses lipid-based mediators called endocannabinoids (eCBs), their synthesizing and degrading enzymes, and two primary receptors (Cota, 2007; Lu and Mackie, 2016). The two best characterized eCBs are 2-arachidonoylglycerol (2-AG) and anandamide (AEA), which act in the central nervous system mainly through two seven transmembrane G protein-coupled receptors (GPCR), namely the cannabinoid type-1 receptor (CB1), one of the most abundant GPCRs in the brain particularly in hippocampal neurons and glial cells, and cannabinoid type-2 receptor (CB2), which in the brain is mostly present in microglia (Busquets-Garcia et al., 2018; Jordan and Xi, 2019). The main endocannabinoid-synthesizing enzymes are N-acyl phosphatidylethanolamine phospholipase D (NAPE-PLD), phospholipase C (PLCγ1) and diacylglycerol lipase (DAGL). Degradation of eCBs is primarily regulated by the fatty acid amide hydrolase (FAAH), the monoacylglycerol lipase (MAGL) and α,β-hydrolase-12 (ABHD12) (Basavarajappa, 2007).

CB1 has been shown to play an essential role in learning and memory (Zanettini, 2011; Busquets-Garcia et al., 2015, 2018) and the ECS is deregulated in several diseases characterized by altered memory processes, including Alzheimer's disease (AD) (Ramirez, 2005), Huntington's disease (Maccarrone et al., 2007), Parkinson's disease (Kim et al., 2005), amyotrophic lateral sclerosis (Bilsland et al., 2006) and multiple sclerosis (Rice and Cameron, 2018).

Interestingly, the ECS was recently shown to be altered in DS mouse models (Lysenko et al., 2014; Navarro-Romero et al., 2019). Lysenko and collaborators found a 50% increase in 2-AG in the total brain of middle-aged Ts65Dn mice (Lysenko et al., 2014) while Navarro-Romero and collaborators showed that the CB1 antagonist rimonabant was able to reverse CD in both Ts65Dn and TgDyrk1A DS mouse models (Navarro-Romero et al., 2019). Even though the two studies are set in distinct temporal and spatial windows; namely middle-aged Ts65Dn mice and total brain samples for Lysenko compared to young Ts65Dn mice and whole hippocampus for Navarro-Romero, the data clearly showed that the ECS and notably the CB1 could be a promising target for innovative therapeutic strategies aimed at improving intellectual disability in DS. However, CB1 is known to have a complex expression pattern, being localized in several brain cell types (neuron/glial cells) and subcellular compartments that have quite opposite behavioral functions through the activation of multiple and selective signaling pathways (Busquets-Garcia et al., 2015, 2018).

Considering the functional importance of the hippocampus (HPC) in memory processes, here we specifically analyzed the expression pattern of ECS components in the HPC of adult male Ts65Dn mice using various molecular approaches. The results show that among all the molecules that constitute the ECS, it is mainly the expression of the CB1 that is altered in the HPC of Ts65Dn mice. More specifically, this alteration targeted the dorsal part of the hippocampus, with a specific segregation within the different populations of neurons.

2. Results

2.1. CB1 encoding gene (Cnr1) expression in the dorsal and ventral hippocampus of Ts65Dn mice

The HPC is a brain structure with functionally distinct areas. The dorsal hippocampus (dHPC) is preferentially involved in memory-related functions (Moser et al., 1995; Ferbinteanu and McDonald, 2001; Pothuizen et al., 2004), whereas the ventral hippocampus (vHPC) has a preferential role in processing stress responses and emotional information (Henke, 1990; Kjelstrup et al., 2002). Navarro and colleagues observed an increase in CB1 protein in the HPC of Ts65Dn mice (Navarro-Romero et al., 2019). However, given the importance of the functional segregation of the HPC in memory processes, we first analyzed the CB1 protein levels in the dorsal and ventral HPC of Ts65Dn mice to see whether a differential gene expression between dorsal and ventral areas might be consistent with memory dysfunctions (Fig. 1). Immunoblotting analysis revealed a significant increase of CB1 protein levels in the dHPC (Fig. 1A) but not in the vHPC (Fig. 1B) of Ts65Dn mice as compared with control littermates (WT).

qRT-PCR analysis with primers targeting both the coding (amplicon 1) and non-coding (amplicon 2) regions of *Cnr1* gene (Fig. 2A), consistently revealed that *Cnr1* mRNA expression was also significantly increased in the dHPC (Fig. 2B) but not in the vHPC (Fig. 2C) of Ts65Dn mice as compared to WT. Neither CB1 mRNA or protein expression was altered in the prefrontal cortex (PFC) of Ts65Dn mice (Fig. S1), which is another key structure underlying the cognitive deficits observed in DS (Rowe et al., 2006). Thus, these results showing a selective increased expression of CB1 in the dHPC are in agreement with a potential role of CB1 supporting CD in Ts65Dn mice (Zanettini, 2011; Busquets-Garcia et al., 2015; Navarro-Romero et al., 2019).

2.2. mRNA expression of ECS components in dHPC and vHPC of Ts65Dn mice

We then went on to investigate the gene expression of ECS enzymes involved in the synthesis and degradation of eCBs in the dHPC and vHPC of Ts65Dn mice (Fig. 3). The eCBs are derived essentially from phospholipids (N-arachidonoyl phosphatidyl ethanolamine, NAPE and phosphatidylinositol 4,5-bisphosphate, PIP2) (Sugiura, 2008). The main enzymes involved in eCB synthesis are the N-arachidonoyl phosphatidyl ethanolamine phospholipase D (NAPE-PLD) for AEA, and the phospholipase C (PLCγ1) and the diacylglycerol lipase (DAGLa/b) for 2-AG (Fig. 3A). In the dHPC, qRT-PCR analysis of mRNAs encoding AEA synthesis enzymes showed a slight (less than 10%) but significant decrease in *Nape-pld* mRNA whereas for 2-AG synthesis a significant increase in *Daglb* transcripts was observed and *Dagla* transcripts showed an opposite trend (Fig. 3B). The degradation of eCBs involved the Fatty acid amide hydrolase (FAAH) that metabolizes AEA into ethanolamine (ETA) and arachidonic acid (AA), whereas the monoacylglycerol lipase (MAGL) converts 2-AG in glycerol and AA, and the α,β-hydrolase-12 (ABHD12) metabolizes 2-AG in AA (Fig. 3A). In the dHPC, the expression of genes encoding AEA and 2-AG degradation enzymes was unaffected (Fig. 3B). In the vHPC, genes encoding enzymes involved both in the synthesis and degradation of AEA and 2-AG were also similar between genotypes (Fig. 3C). In addition, we found that the mRNA expression of *Cnr2*, encoding for the CB2 receptor, was unaffected both in the dorsal and ventral HPC of Ts65Dn mice as compared to control littermates (Fig. 3B and C).

2.3. Levels of endocannabinoids 2-AG and AEA in dHPC and vHPC of Ts65Dn mice

We also determined levels of the main eCBs (AEA and 2-AG) in the dorsal and ventral HPC of Ts65Dn mice using mass spectrometry analysis. In agreement with the mRNA expression analysis, results showed

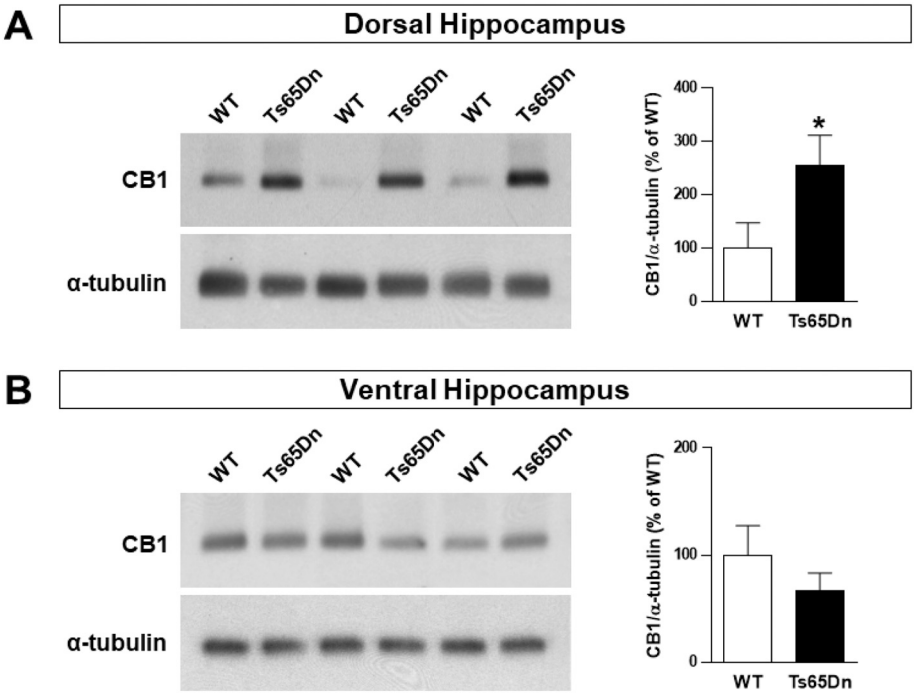

Fig. 1. CB1 protein expression is increased in the dorsal hippocampus of male Ts65Dn mice. CB1 measured by Western Blot in the dorsal ($n = 8$) (A) and ventral (n = 8–10) (B) hippocampus of Ts65Dn mice. Males of both genotypes were used. α-Tubulin was used as a loading control. X-ray films were quantified by densitometry (OD). $^*p < 0.05$ compared to control WT group. Plotted values are means ± sem.

that AEA, but not 2-AG, was decreased in the dHPC of Ts65Dn mice as compared to control littermates (Fig. 4A). Conversely, analysis of the vHPC showed no differences between Ts65Dn and WT mice (Fig. 4B).

2.4. Distribution of Cnr1 mRNA-expressing cells in subpyramidal areas of the dHPC in Ts65Dn mice

The HPC is divided into distinct subfields referred to as *CA1*, *CA2/CA3* and *DG* (Dentate Gyrus) including the GABAergic- and glutamatergic neuron-enriched areas that play a prominent role in some of the HPC-mediated behaviors (Abrous et al., 2005; Martin and Clark, 2007). CB1 is not equally distributed within these hippocampal areas, showing high levels of expression in GABAergic interneurons and low levels of expression in glutamatergic cells and astrocytes (Marsicano and Lutz, 1999; Kawamura et al., 2006; Kano et al., 2009; Han et al., 2012). Having found a selective increase in CB1 expression in the dHPC of Ts65Dn (Figs. 1 and 2), we therefore investigated whether *Cnr1* mRNA expression was different within hippocampal areas by using double fluorescent *in situ* hybridization (D-FISH) to label the mRNAs of CB1 and of glutamic acid decarboxylase 65 kDa and 67 kDa (GAD), a marker of GABAergic neurons (Houser and Esclapez, 1994). *Cnr1* mRNA was significantly increased in GABAergic interneurons referred to as GAD-positive cells in *CA1-LMol*, *CA3-SLu* and *DG-Po* layers of Ts65Dn mice compared to control littermates (Fig. 5A–E). Consistent with previous studies (Chakrabarti et al., 2010), the number of GAD-expressing cells was increased in Ts65Dn mice compared to control littermates (Fig. 5F). The decreased percentage of CB1-GAD-positive cells over total GAD positive cells in Ts65Dn mice compared to control littermates indicated that the proportion of GABA neurons expressing CB1 is significantly lower than the population of GABA neurons not expressing CB1 in Ts65Dn mice (Fig. 5G), suggesting that the inhibitory control of CB1 on GABAergic neurons might be reduced in the dHPC of Ts65Dn mice compared to control mice. However we found that the intensity of *Cnr1* mRNA expression in GABAergic neurons was not different between Ts65Dn and WT mice, indicating that the number of *Cnr1* transcripts in GABAergic neurons is similar between the two genotypes (Fig. 5H). No differences were found in the vHPC (data not shown).

2.5. Pattern of Cnr1 mRNA-expressing cells in CA1/CA3 pyramidal and DG granular areas of dHPC in Ts65Dn mice

FISH analysis revealed that the expression levels of *Cnr1* mRNAs expressed by pyramidal neurons were largely decreased in the pyramidal layers (*Py*) in *CA1* and *CA3* and in the granular layer (*Gr*) in *DG* of Ts65Dn mice compared to control littermates (Fig. 6). No differences were found in the vHPC (data not shown).

3. Discussion

DS, a genetic disorder caused by trisomy of the human chromosome 21 (HSA21), is responsible for the dosage imbalance of multiple genes that are responsible notably for hippocampal-dependent learning and memory deficits (Dierssen, 2012; Antonarakis, 2017). The ECS has also been shown to play a crucial role in hippocampal cognitive-related functions (Marsicano and Lafenêtre, 2009; Jacob et al., 2012). In this study, we therefore explored the ECS within the HPC of Ts65Dn mice as a relevant target system that could be affected in DS. Ts65Dn mice showed an alteration of the expression of CB1 in the dorsal part of the HPC and a specific distribution of CB1 within the different cell populations that constitute the dHPC.

3.1. CB1 mRNA and protein expression and localization in the HPC of Ts65Dn mice

Using several molecular approaches, our data showed a selective increase in *Cnr1* mRNA and CB1 protein expressions in the dHPC, but not in the vHPC and PFC of male Ts65Dn mice. These results suggest that the CB1 selective increase restricted to the dHPC could support the cognitive impairment of Ts65Dn mice. Navarro and colleagues reported no difference in CB1 expression at mRNA level and a weak increase at protein level in the whole HPC of Ts65Dn mice, probably reflecting a dilution effect when studying structure-wide (Navarro-Romero et al.,

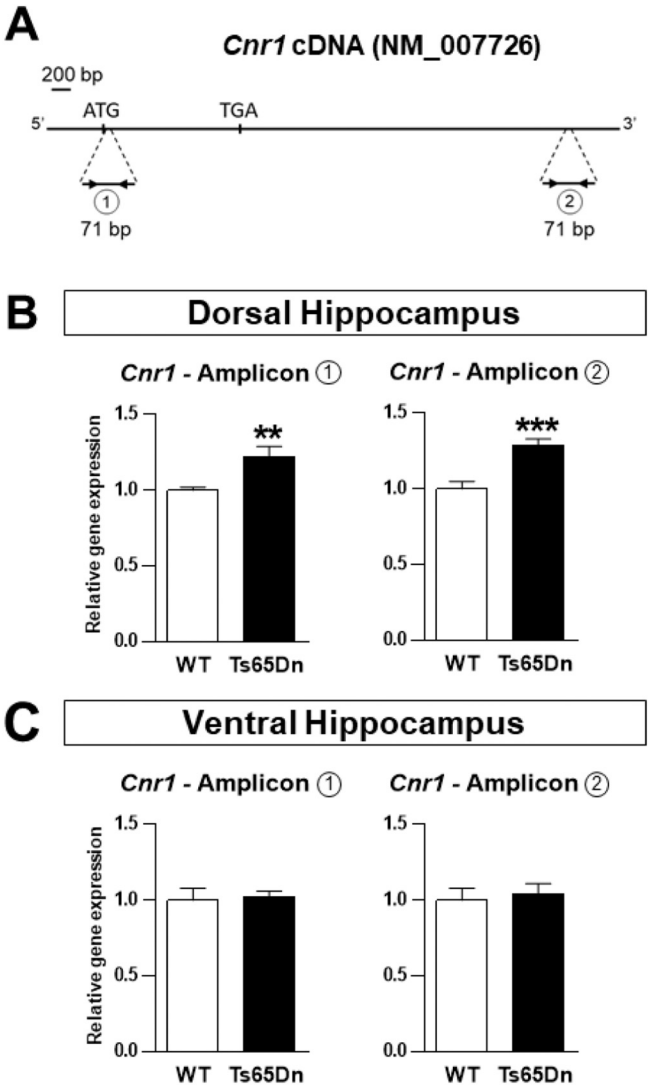

Fig. 2. *Cnr1* gene expression is increased in the dorsal hippocampus of male Ts65Dn mice. Location of qPCR primers used for quantification of *Cnr1* cDNA (A). Primer pair 1 amplifies an amplicon in the N-terminus encoding sequence whereas primer pair 2 amplifies an amplicon in the 3′ non coding region. *Cnr1* relative gene expression level expressed as fold change normalized to control WT mice gene expression in the dorsal (B) and ventral (C) hippocampus. $n = 11$ control and $n = 8$ Ts65Dn mice were used for each hippocampal structure. $^{**}p < 0.01$, $^{***}p < 0.001$ compared to control WT group. Plotted values are means ± sem.

2019).

Several other genes related to the main components of ECS were investigated, namely the CB2, the eCB degradation enzymes (ABHD12, FAAH and MAGL), and the eCB biosynthesis enzyme (NAPE-PLD, PLCγ1 and DAGLα/β). There was no change in the expression of these ECS-related genes in the Ts65Dn mice in the vHPC. In the dHPC of Ts65Dn mice, we found a small but significant decrease in the *Nape-pld* encoding gene responsible for AEA synthesis, together with a decrease in AEA level, whereas 2-AG remained unaltered. The increase in 2-AG reported by Lysenko and colleagues can be explained by the age of Ts65Dn mice and their characteristic to further develop Alzheimer's disease-like symptoms (Hyde et al., 2001; Hunter et al., 2004). Indeed, recent study showed in patients with AD a deregulation of the ECS and in particular an increase in plasma 2-AG (Altamura et al., 2015). Interestingly, it has been hypothesized that AEA and 2-AG differentially regulated synaptic processes operating in tonic and phasic modes, respectively. AEA as a 'tonic' signaling molecule would regulate basal synaptic transmission, whereas 2-AG as a 'phasic' signaling molecule being released upon stimulation would mediate specific forms of synaptic plasticity (Ahn et al., 2008; Katona and Freund, 2012). Therefore, we cannot rule out that the decrease in AEA could compensate for the CB1 overexpression in order to regulate CB1 'tonic' activity in the dHPC of Ts65Dn mice. However, this simple dichotomy is complicated by the specific expression and regionalization pattern of the CB1 receptor within the dHPC. Indeed, using FISH we found higher levels of CB1 in the *LMol* and *SLu* layers of *CA1* and *CA3* areas and in the *Po* layer of the dentate gyrus as compared to control mice, together with significantly lower levels of expression in the *Py* layer of *CA1* and *CA3* and the granule cell layer of the dentate gyrus. This complex pattern of alterations in the levels of *Cnr1* mRNA in different subregions of the dHPC may be linked to specific mechanisms, including: i) a positive transcriptional loop for CB1 expression (Laprairie et al., 2012), ii) a dosage imbalance of certain transcription factors (Antonarakis, 2017), or iii) the consequence of cell density and migration alterations during embryologic development (Moser and Moser, 1998; Fanselow and Dong, 2010).

3.2. Functional consequences of CB1-related alterations

The alteration of CB1 expression could have a powerful impact on neuronal activity as a neurobiological substrate underlying cognitive deficit impairments. HPC and PFC brain structures, two brain regions richly expressing CB1 (Riedel and Davies, 2005) are both involved in the regulation of memory processes (Preston and Eichenbaum, 2013; Chao et al., 2020). It is now well admitted that general overinhibition observed in Ts65Dn mice is linked to an excitation–inhibition imbalances caused by abnormal circuitry, thus explaining intellectual disability observed in DS (Belichenko et al., 2007; Souchet et al., 2015). Interestingly, recent data investigating links between neural circuitry and memory deficiencies have shown that Ts65Dn mice displayed abnormal PFC-HPC functional connectivity that can be associated with learning and memory impairments (Alemany-González et al., 2020). Therefore, it is plausible that the CB1 expression imbalance between dHPC-PFC brain structures we observed in Ts65Dn mice may contribute to the neural mechanism disturbances underlying this synaptic inhibition and the related cognitive deficits.

In addition, CB1 activity could be further increased as a result of its constitutive activity (Fong, 2014). Since the role of CB1 signaling is to suppress presynaptic transmitter release leading to inhibition of the presynaptic neurons to maintain excitation/inhibition homeostasis (Silva-Cruz et al., 2017), overactivity of the receptor could tilt the balance in favor of inhibition, exacerbating the DS pathology. Additionally, the CB1 antagonist rimonabant has been shown to restore the excitatory tone and LTP in the hippocampus, in turn improving the cognitive performance of Ts65Dn mice (Navarro-Romero et al., 2019). Altered glutamatergic/GABAergic cell proportion also supports the excitatory/inhibitory imbalance hypothesis to explain DS cognitive impairments (Hernández-González et al., 2014). For instance, the number of specific subpopulations of GABAergic interneurons was shown to be altered in the HPC of Ts65Dn mice such as interneurons expressing calcium binding proteins (calbindin D-28k, calretinin and parvalbumin) or neuropeptides (cholecystokinin (CCK), neuropeptide Y (NPY), vasoactive intestinal peptide (VIP), somatostatin). The general picture is an increase in the number of inhibitory neurons in *CA1* and *CA3* subregions of the HPC, notably calbindin D-28k, calretinin, NPY, VIP and basket expressing interneurons whereas parvalbumin, CCK and somatostatin ones were not affected (Hernández-González et al., 2014; Mojabi et al., 2016). Furthermore, double *in situ* hybridization study has confirmed that CB1 is also expressed in distinct GABAergic subpopulations, highly in CCK-positive and parvalbumin-negative types of interneurons (basket cells) and, to a lower extent, to the calbindin D28k-positive inhibitory interneurons (Marsicano and Lutz, 1999). As such, there is not a perfect match between increased GABAergic interneurons subpopulations and

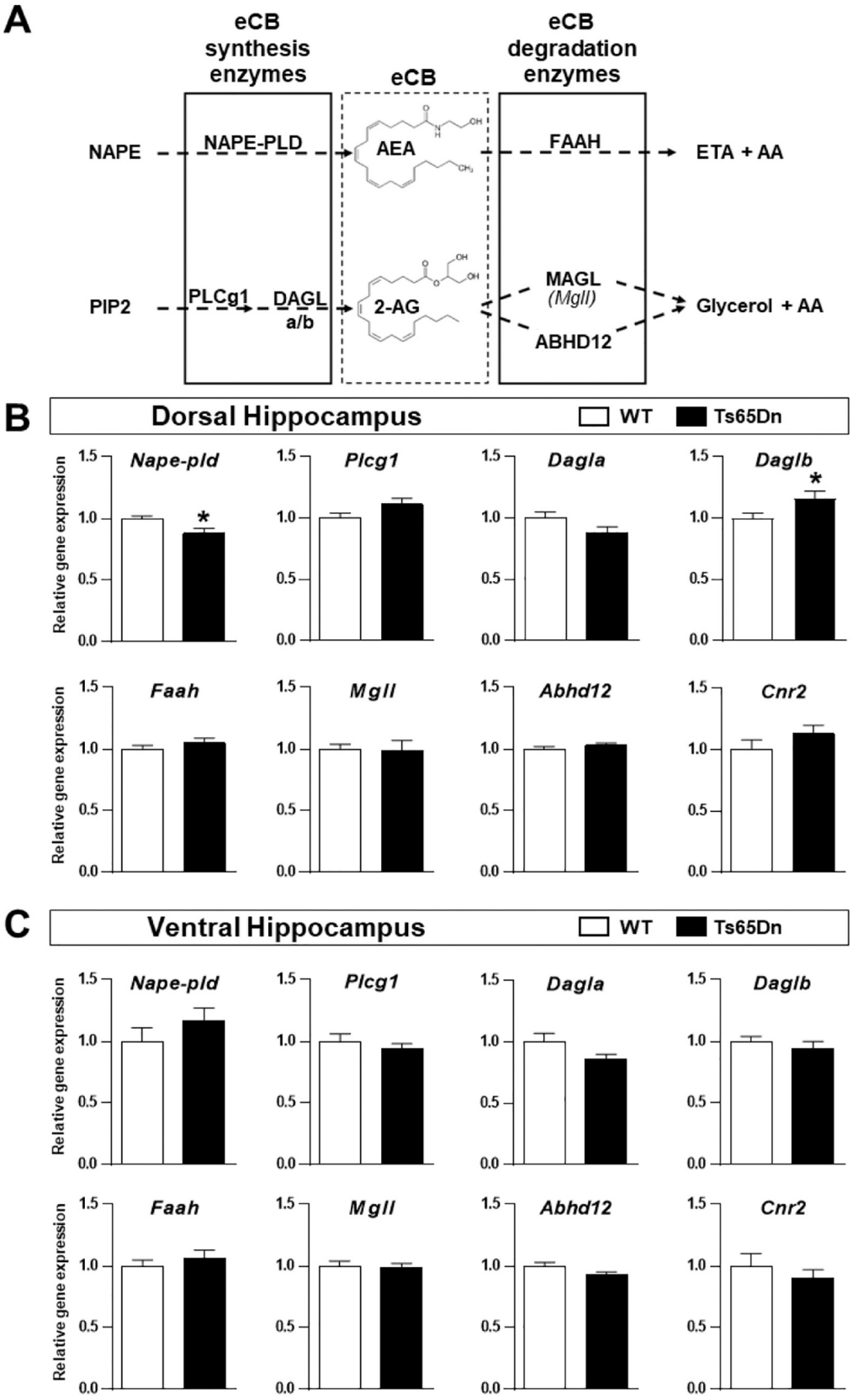

Fig. 3. Expression profile of genes belonging to the endocannabinoid system in the hippocampus of male Ts65Dn mice. Diagram of the canonic pathway for endocannabinoid (eCB, anandamide, AEA and 2-arachidonoylglycerol, 2-AG) synthesis and degradation (A). Relative gene expression of *Abhd12* (α,β-hydrolase domain containing 12), *Dagla* and *Daglb* (diacylglycerol lipase alpha and beta), *Faah* (fatty acid amide hydrolase), *Mgll* (monoacylglycerol lipase), *Nape-pld* (N-acyl-phosphatidylethanolamine phospholipase D), *Plcg1* (phospholipase C γ1) and *Cnr2* (CB2) expressed as fold change normalized to control WT mice gene expression in the dorsal (B) and ventral (C) hippocampus. $n = 11$ control and $n = 8$ Ts65Dn mice were used for each hippocampal structure. NAPE, N-acyl-

phosphatidylethanolamine; PIP2, phosphatidylinositol 4,5-bisphosphate, AA, arachidonic acid; ETA, ethanolamine. *$p < 0.05$ compared to control WT group. Plotted values are means ± sem.

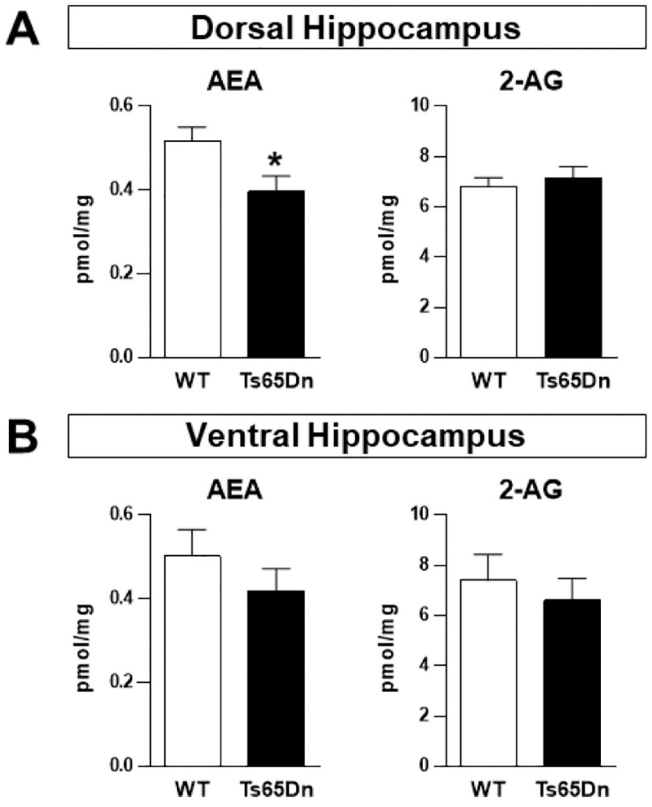

Fig. 4. Endocannabinoids dosage in the dorsal and ventral hippocampus of male Ts65Dn mice. Levels of Anandamide (AEA) and 2-arachidonoylglycerol (2-AG) were measured in the dorsal (A) and ventral (B) hippocampus of Ts65Dn mice using liquid chromatography–tandem mass spectrometry. $n = 8–9$ control and n = 8–9 Ts65Dn mice were used for each hippocampal structure. *$p < 0.05$ compared to control WT group. Plotted values are means ± sem.

those expressing CB1 in Ts65Dn mice. However, as the majority of high CB1-expressing cells are GABAergic interneurons their increase would be sufficient to elicit increased GABA signaling that in turn would result in a decreased general excitability of pyramidal neurons, preventing LTP and thus affecting hippocampal-related tasks (Kleschevnikov et al., 2004).

Furthermore, we cannot exclude a possible alteration in the expression of astroglial CB1, which can only be detected by electron microscopy because of its extremely low expression in this cell type (Han et al., 2012). Indeed, activation of astroglial CB1 by exogenous cannabinoids has been shown to be associated with the induction of astroglia-dependent hippocampal LTD *in vivo* at *CA3-CA1* synapses to mediate spatial working memory impairment (Han et al., 2012). Finally, at an even compartmentalized level, activation of mitochondrial CB1 by Δ^9-tetrahydrocannabinol (THC), through a decrease in mitochondrial metabolism and thus a reduction in hippocampal synaptic transmission, leads to a decrease in memory performance (Hebert-Chatelain et al., 2016). Interestingly, several studies have revealed that mitochondrial dysfunctions are strongly associated with DS (Lott, 2012; Perluigi and Butterfield, 2012; Helguera et al., 2013).

3.3. Ts65Dn mice as a reliable model to explore ECS alteration in DS

Creating a suitable mouse model of DS has proven challenging due to the length of the triplicated sequence (35 Mb) of HSA21, but also because its orthologs in mouse map span segments of three different chromosomes: Mmu16, Mmu17, Mmu10 (Davisson et al., 1990).

In our study, we used the well-characterized Ts65Dn mouse model of DS. Ts65Dn mice were created after X-ray irradiation and carry a genomic segment with 122 genes homologous to HSA21 resulting from Mmu16 distal region translocation into Mmu17 centromere (Davisson et al., 1993). These mice are trisomic for ~56.5% of the HSA21 syntenic region on mouse as they contain an additional set of triplicated non-related HSA21 genes which therefore adds a supplementary level of complexity in the evaluation of DS-related phenotypes (Duchon et al., 2011). To correct for this imperfection, other DS mouse models displaying higher construct validity than Ts65Dn mice have been developed using Cre/LoxP-mediated long-range chromosome engineering thus carrying a well-defined segmental duplication without additional chromosomal rearrangement (Herault et al., 2017). Notably, the Dp(16)1Yey/+ mice were generated by duplication of the entire 22.9 Mb HSA21 syntenic region on mouse chromosome 16 (Li et al., 2007) or the TTS mice a 'triple trisomic' model which carries the duplications of all three mouse regions homologous to HSA21 (Belichenko et al., 2015). With some phenotypes similar to those of patients with Down syndrome, these mouse models might also represent alternative tools to further understand the molecular and cellular mechanisms of DS. However, due to heart defects, approximately 30% of Dp(16)1Yey/+ and TTS offspring die shortly after birth, and only 12.5% of TTS offspring carry triple trisomy (Li et al., 2007; Yu et al., 2010), which may undermine their preclinical use.

Yet, Ts65Dn mice still exhibit one of the best face validity, recapitulating most of the features of DS, including neuronal abnormalities and cognitive deficits (Aziz et al., 2018). For these reasons, and due to its relatively high fertility, Ts65Dn mice are to date the main model used for preclinical studies to investigate the cognitive deficits of DS, with many studies reporting the reversal of the phenotype by using different drugs and small molecules (Gupta et al., 2016). To complete our findings showing a significant increase in CB1 in the dHPC, further analyses investigating ECS and in particular CB1 in different DS mouse models with triplicated segments different from those of Ts65Dn mice should be performed. For example, a similar strategy could be performed in the TgDyrk1A mouse model in which the kinase Dyrk1A is overexpressed (Altafaj et al., 2001), that displays a CB1 increase in the whole HPC (Navarro-Romero et al., 2019). In addition, it would be worth completing this study with a meta-analysis of the different transcriptomic databases (*i.e.* proteomic, microarray and RNAseq datasets) available on DS (Duchon et al., 2021; Toma et al., 2021), both in the different mouse models and in humans with DS. However, keeping in mind that the complex regulation of the CB1 expression subregionalized within the HPC suggests to be cautious when analyzing proteomic and RNA datasets based on structure-wide.

3.4. CB1 as a potential therapeutic target for cognitive improvement in DS

Finding a potential drug that improves CD available to DS subjects is a challenging issue. To date, among the different compounds tested, only the antioxidant epigallocatechin-3-gallate reached phase 3 clinical studies for CD (ClinicalTrials.gov Identifier: NCT01699711 and NCT01394796, phase 2 completed). Among the diverse brain target systems that were shown to improve hippocampal-dependent CD in preclinical mouse models, recent works suggested that the ECS could be a potential therapeutic target in DS (Lysenko et al., 2014; Navarro-Romero et al., 2019). Administration of JZL184, a MAGL inhibitor blocking the degradation of 2-AG, to aged Ts65Dn mice expressing Alzheimer's disease symptomatology (Hobson-Rohrer and Samson-Fang, 2013) was reported to improve long-term memory and synaptic

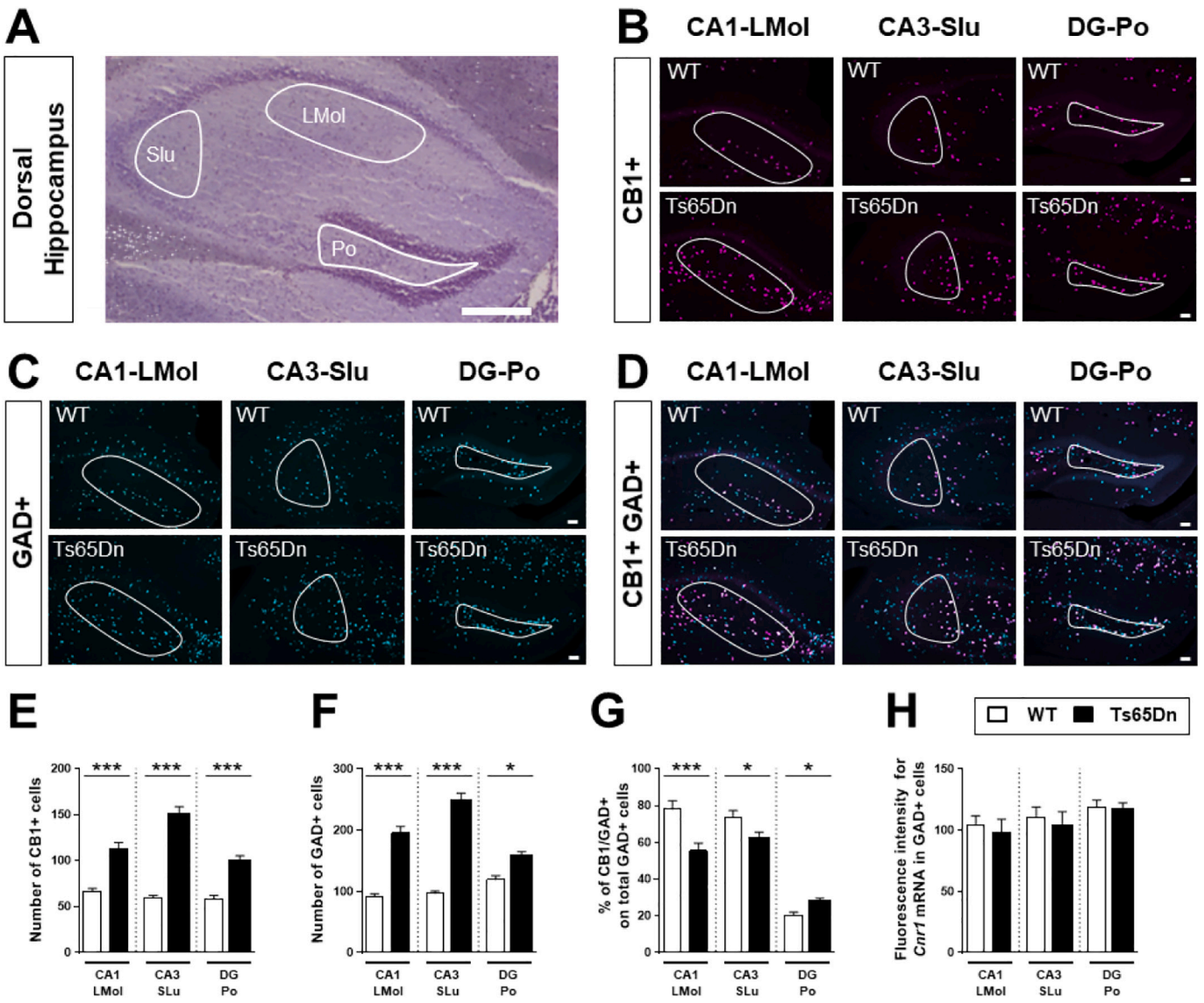

Fig. 5. CB1 distribution in subpyramidal areas of the dorsal hippocampus of male Ts65Dn mice. Representative bright field image showing GABAergic neurons-enriched areas radiatum and lacunosum moleculare strata (*LMol*) in *CA1*, stratum lucidum (*SLu*) in *CA3* and polymorph dentate gyrus (*Po*) (A). The area delineated by the white lines is quantified. Scale bar, 100 μm. Representative images showing double fluorescent *in situ* hybridization (D-FISH) of *Cnr1* mRNA (purple) (B), *Gad65/67* mRNA (GAD, green) (C) and merges (white) of the two signals (D) are shown in the dorsal hippocampus of control WT ($n = 5$) and Ts65Dn (n = 5) mice. Scale bar, 100 μm. Quantification of the number of CB1 positive spots (E), of GABAergic positive cells (F) and the percentage of CB1 in GABAergic neurons over the total number of GABAergic neurons (G) in the different layers of the dorsal hippocampus. Integrated density of CB1 expression in GABAergic neurons in the *CA1-LMol*, *CA3-SLu* and *DG-Po* (H) is shown. $^{*}p < 0.05$, $^{**}p < 0.01$, $^{***}p < 0.001$ compared to control WT group. Plotted values are means ± sem. (For interpretation of the references to colour in this figure legend, the reader is referred to the web version of this article.)

plasticity (Lysenko et al., 2014). However, administration of JZL184 to C57Bl/6 mice was shown to induce addictive-like effects similar to THC, including analgesia, hypothermia, and hypomotility (DeLong et al., 2010), suggesting that this compound cannot be used in clinical trials. Recently, pharmacological inhibition of CB1 using the antagonist rimonabant was shown to restore memory deficits in Ts65Dn mice providing evidence that CB1 is a relevant target for the improvement of CD associated with DS (Navarro-Romero et al., 2019). Unfortunately, CB1 receptor antagonists such as rimonabant inhibiting the entire CB1 activity are clinically unsuitable as a CD therapy due to their adverse effects (Christensen et al., 2007; Seely et al., 2012). Another potential treatment option to consider is the use of the neurosteroid pregnenolone (PREG). PREG has been recently shown to act as a potent endogenous allosteric signal-specific inhibitor of CB1 protecting the brain from cannabis intoxication (Vallée et al., 2014). In addition, PREG has been shown to block a wide spectrum of THC-induced endophenotypes typically associated with psychotic-like states, including impairments in cognitive functions, somatosensory gating and social interaction (Busquets-Garcia et al., 2017), revealing that signal-specific inhibitors mimicking PREG effects can be considered as promising new therapeutic tools to improve CB1-mediated CD.

In conclusion, our data show a selective increase in CB1 expression and distribution according to GABAergic and glutamatergic neuronal subtypes within distinct subfields of the dHPC thereby likely determining the ability of eCBs to deregulate the excitatory and inhibitory CB1-mediated balance in specific cell subpopulations in Ts65Dn mice. Supporting our results, preprint data from Vázquez-Oliver and colleagues deposited in BioRxiv online archive (Vázquez-Oliver et al., 2021) showed that CB1 expression is enhanced in hippocampal post-mortem samples of human DS subjects obtained from the Neurological Tissue Bank (Biobanc-Hospital Clínic-IDIBAPS, Barcelona, Spain).

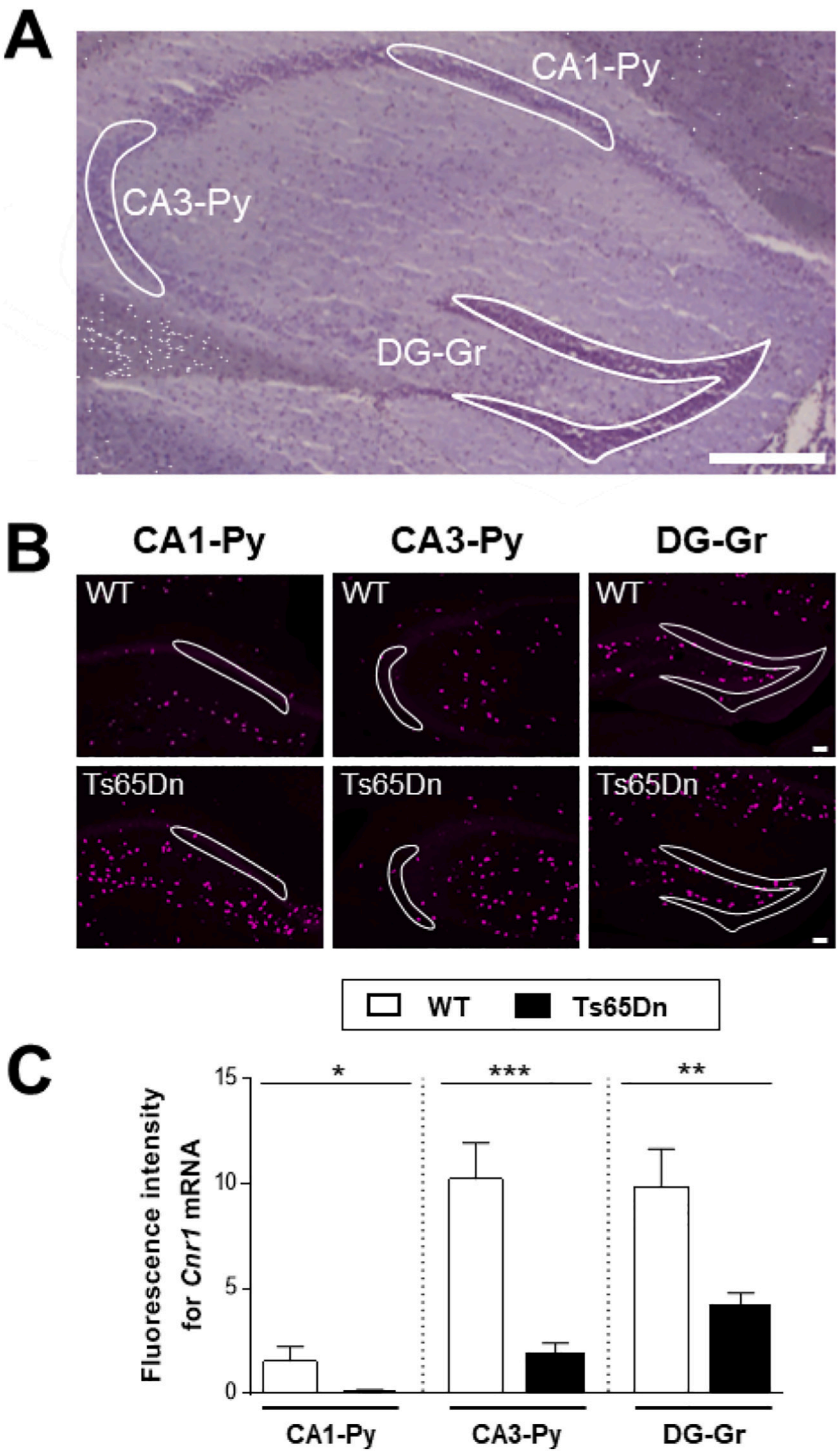

Fig. 6. CB1 distribution in pyramidal neurons in the dorsal hippocampus of male Ts65Dn mice. Representative bright field image showing pyramidal layers (*Py*) of *CA1* and *CA3*, and granular layer of dentate gyrus (*Gr*) (A). The area delineated by the white lines is quantified. Scale bar, 100 μm. Representative images showing fluorescent *in situ* hybridization (FISH) of *Cnr1* mRNA (purple) (B) in the dorsal hippocampus of control WT ($n = 5$) and Ts65Dn (n = 5) mice. Scale bar, 100 μm. Integrated density of CB1 expression in pyramidal neurons in *CA1-Py*, *CA3-Py*, *DG-Gr* (C) is shown. $^{*}p < 0.05$, $^{**}p < 0.01$, $^{***}p < 0.001$ compared to control WT group. Plotted values are means ± sem. (For interpretation of the references to colour in this figure legend, the reader is referred to the web version of this article.)

4. Materials and methods

4.1. Experimental animals

Three to four month-old male Ts65Dn mice and control (WT) littermates were used. Ts65Dn mice were created by mating female carriers of 17^{16} chromosome (B6C3H-Ts65Dn) with B6EiC3HF1 hybrid males, obtained by crossing C57BLr/6JEi with C3Hr/HeSnJ mice (Reeves et al., 1995). Four different batches of mice were used in these experiments: Western blot ($n = 8$–10 *per* genotype), qRT-PCR ($n = 11$ control and n = 8 Ts65Dn mice), eCB measurement (n = 8–9 *per* genotype). Fluorescence *in situ* hybridization (FISH) experiments were performed on Ts65Dn and control littermate male mice ($n = 5$ mice *per* genotype), and on one full CB1 knockout (CB1-KO) male mouse as probe control (Marsicano et al., 2002). Experiments were performed during the light phase (from 7 am to 7 pm) and animals were kept in collective cages under a 12 h light/dark cycle under controls (22 °C, 60% humidity) with water and food (A04-10 pellets, Scientific Animal Food & Engineering) *ad libitum*. Animals were acclimated to the housing conditions for two weeks prior to the start of the experiments; they were bred and PCR-genotyped in the Magendie Neurocentre Institute.

4.2. Sacrifice for molecular analysis

Each mouse was sacrificed by decapitation. The prefrontal cortex and dorsal and ventral hippocampus were collected, rapidly frozen and kept at −80 °C until analyses.

4.3. Surgery for in situ hybridization analysis

Mice were anesthetized by intraperitoneal injection (IP) of a mixture of pentobarbital (Exagon, 200 mg/kg) and the anesthetic lidocaine (Lurocaine® 20 mg/ml) purchased from Centravet (Dinan, France) at the dose of 10 µl/g. The infusion was delivered through the left ventricle with tampon phosphate-buffered saline (PBS 0.1 M, pH = 7.4) in heparin (5000 UI/L) for 2 min followed by 4% formaldehyde dissolved in PBS (0.1 M, pH = 7.4) for 5 min. After infusion, the brains were removed from the skull and post-fixed in the same fixative solution for 24 h at 4 °C. The following day, the brains were embedded with 30% sucrose for 3 days, frozen and kept at −80 °C. Serial brain coronal cryosections were cut at the cryostat (30 µm, Microm HM 500 M, Microm Microtech), collected on anti-freeze solution (containing: glycerol 20%, ethylene glycol 30%, NaH_2PO_4, 0.23 M and $NaH_2PO_4{\cdot}2(H_2O)$, 0.23 M) and stored at −20 °C.

4.4. Protein extraction

Frozen brain tissues were homogenized with a Precellys 24 (Bertin Technologies, Montigny-le-Bretonneux, France) using AlphaLISA Sure Fire Ultra Lysis Buffer (1×); 137 mM NaCl, 2.7 mM KCl, 8.1 mM Na_2HPO_4, 1.7 mM KH_2PO_4, 2.5 mM Sodium Pyrophosphate, 10 mM NaF, 2 mM Sodium Orthovanadate, 0.2% Triton X-100, 0.05% Proclin 300, pH 7. The homogenization was done at 5000 rpm, twice for 30 s plus a 10 s break. Protein concentration was determined using a Direct Detect Infrared Spectrometer (Merck). Proteins were diluted in RunBlue LDS Sample Buffer (Euromedex) and were heat-denatured for 5 min at 100 °C then subjected to Western blot analysis.

4.5. Western analysis

10 µg of total proteins were separated by Mini Protean TGX precast electrophoresis gels 4–15% (Bio-Rad Laboratories, USA) at 200 V constant for 50 min in the Tris-Glycine SDS Buffer (Euromedex, France). Proteins were transferred onto PVDF membranes (Immobilon P, Millipore, USA). The transfer was performed at 4 °C 1 h in Tris/glycine/10% methanol buffer at 100 V. The membrane was first blocked for 60 min at room temperature in TBS/T-milk, Tris-buffered saline (TBS) containing 5% dry powdered non-fat milk, 0.05% Tween 20. Later, the membrane was incubated overnight at 4 °C in the same TBS/T-milk solution containing an anti-CB1 rabbit polyclonal antibody (# ab23703, Abcam, France) at 1/5000 dilution. The membranes were then washed twice for 7 min with TBS/T and incubated 1 h at room temperature in TBS/T containing anti-rabbit IgG-HRP (# 7074S, 1/5000, Cell Signaling Technology, USA) secondary antibody at 1/5000 dilution. After TBS/T and TBS washings, the signal was revealed following chemiluminescent detection (Immobilon Forte Western HRP Substrate, Millipore, USA). The X-ray films (BioMax MR film, Kodak, USA) used to detect the chemiluminescent signal, were scanned in transmission mode using a GS-800 scanner (Bio-Rad Laboratories, CA, USA) following the manufacturer's instructions. The same membrane was reused for the control hybridization with the monoclonal anti α-Tubulin (#NR356, 1/50000, Amersham, USA) and revealed with the anti-mouse IgG-HRP secondary antibody (#7076, 1/20000, Cell Signaling Technology, USA) (Bouarab et al., 2021).

4.6. Endocannabinoid measurements

Measurements of AEA and 2-AG were carried out as previously described (Matias et al., 2012). Brain structures were homogenized and extracted with chloroform/methanol/Tris-HCl (50 mM, pH 7.5, 2:1:1, vol/vol) containing internal deuterated standard (AEA-d4 and 2-AG-d5), and the dried lipid extract was purified using solid-phase extraction (SPE C18 Agilent, France). Mass spectral analyses were conducted on a TSQ Quantum triple quadrupole instrument (Thermo-Finnigan) equipped with an atmospheric pressure chemical ionization source and operating in positive ion mode. AEA and 2-AG levels were determined by isotope-dilution using a calibration curve. Endocannabinoid levels were then normalized by the weight of fresh tissue.

4.7. Quantitative real time polymerase chain reaction (qRT-PCR)

Total RNA was extracted using a standard acid guanidinium thiocyanate/phenol/chloroform protocol and purified by incubation with Turbo DNA-free (Fischer Scientific) (Chomczynski and Sacchi, 1987). The purity and concentration of RNA samples were determined from OD260/280 readings using ND1000 UV spectrophotometer (Thermo Scientific) and RNA integrity was determined by capillary electrophoresis using the RNA 6000 Nano LabChip kit run on the Bioanalyzer 2100 (Agilent Technologies). cDNA was synthesized from 2 µg of RNA with Maxima RT (Fischer Scientific) using a mix of random primers (Fischer Scientific) and oligo(dT)18 primers (Fischer Scientific). Transcript-specific primers were generated with Primer Express software (Applied Biosystems) based on GenBank sequence information, verified by NCBI BLAST search, and custom synthesized (Eurogentec). In addition, primers are designed to respect MIQE parameters (Bustin et al., 2009). The sequences of all primer pairs can be found in Table 1. Each primers set was tested by melting curve analysis and gel electrophoresis for the absence of primer-dimer artifacts and multiple products. Amplification efficiency of each set was determined by qPCR, using repetitive dilution series of cDNA. Only primers with an efficiency of ~2 were used.

The quantification cycle (Cq) value was measured using the second derivative maximum method implemented in the LightCycler® Real-Time PCR System (Roche Applied Science). For each primer set, a no-template control was performed, and Cq values with a difference < 6 cycles were discarded. PCR conditions and LightCycler® 480 SYBR Green I Master mix (Roche Applied Science) were used in a reaction of 10 µl, using transcript-specific primers (0.6 µM) and 2 µl cDNA equivalent to 4 ng total RNA input. An initial denaturation step at 95 °C for 5 min was followed by 45 cycles of 95 °C for 15 s, 61 °C for 15 s. The PCR data were exported and analyzed with the IT tool GEASE (Gene Expression Analysis Software Environment) developed at the Magendie Neurocentre. Relative gene expression levels of the transcripts were analyzed using the comparative Cq method (2-ΔΔCT) implemented in GEASE, as detailed by Livak and Schmittgen (2001) using two reference genes for normalization. Based on twelve genes selected as potential reference genes, we used the geNorm software package (Vandesompele et al., 2002) to find the most stable genes and to determine how many reference genes should be used as a minimum for normalization. The reference genes used for the analysis were *Eef1a1* (eukaryotic translation elongation factor 1 alpha 1), *Gapdh* (glyceraldehyde-3-phosphate dehydrogenase), *Nono* (non-POU-domain-containing, octamer binding protein), *Ppia* (peptidylprolyl isomerase A), *Sdha* (succinate dehydrogenase complex flavoprotein subunit A) and *Tuba4a* (tubulin, alpha 4A).

4.8. Fluorescent in situ hybridization (FISH)

In order to analyze the distribution of CB1-positive cells and to evaluate the CB1-positive cells in GABAergic neurons within the dorsal Hippocampus (dHPC), ventral Hippocampus (vHPC), we performed double fluorescent *in situ* hybridization (D-FISH). Labeling of *Cnr1* mRNA and of glutamic acid decarboxylase 65 kDa plus 67 kDa (GAD65/GAD67) mRNA for GABAergic neurons was performed as described below (Marsicano and Lutz, 1999; Terral et al., 2019). For each

Table 1
Primer sequences.

Transcript	Forward primer	Reverse primer	Amplicon size	Accession N°
Cnr1 Amplicon 1	5′-GTCGATCTTAGACGGCCTTGC-3′	5′-TTGAGCCCACGTAGAGGAGGT-3′	71 bp	NM_007726
Cnr1 Amplicon 2	5′-TCAGTTGCTGTGGAATCTTTAAAAA-3′	5′-CTGATCGCAGGACCCCTAGA-3′	71 bp	NM_007726
Cnr2	5′-TGTGTGGGTCAGGCATGCT-3′	5′-CACTTGCTTGGTACACCGGAA-3′	71 bp	NM_009924
Abhd12	5′-GCCTTCCTCAGCTGTCCCT-3′	5′-GAAGTGCAGATCCAGGTGCC-3′	72 bp	NM_024465
Dagla	5′-GGTCCTGCTCGTGCTGTCTC-3′	5′-TGCAGCCACAACAGTTGTCTTC-3′	84 bp	NM_198114
Daglb	5′-TTGTAGGCCAGCCCATGG-3′	5′-GCCTTGCAGACCCACTAAGG-3′	71 bp	NM_144915
Faah	5′-CGGCCATCTTGAGGGTCAT-3′	5′-GGCTGCAGTGCAGAGCG-3′	71 bp	NM_010173
Mgll	5′-TCACACTTCCCTTTCTCTCCTGAT-3′	5′-GTGACAAACCAGTGACCCACTGT-3′	71 bp	NM_011844
Nape-pld	5′-GAACGGCCTTGGCATAGCT-3′	5′-GACCAGACCACAAATCACATGG-3′	72 bp	NM_178728
Plcg1	5′-CGGCAAGCTGCAAGTTTTG-3′	5′-AGGTTGCTGGTGTGGCTTATTT-3′	71 bp	NM_021280
Eef1a1	5′-TGAACCATCCAGGCCAAATC-3′	5′-GCATGCTATGTGGGCTGTGT-3′	71 bp	NM_010106
Gapdh	5′-TCAAGAAGGTGGTGAAGCAG-3′	5′-TGGGAGTTGCTGTTGAAGTC-3′	100 bp	NM_008084
Nono	5′-CTGTCTGGTGCATTCCTGAACTAT-3′	5′-AGCTCTGAGTTCATTTTCCCATG-3′	72 bp	NM_023144
Ppia	5′-CAAATGCTGGACCAAACACAA-3′	5′-GCCATCCAGCCATTCAGTCT-3′	71 bp	NM_008907
Sdha	5′-TACAAAGTGCGGGTCGATGA-3′	5′-TGTTCCCCAAACGGCTTCT-3′	74 bp	NM_023281
Tuba4a	5′-CCACTTCCCCTTGGCTACCTA-3′	5′-CCACTGACAGCTGCTCATGGT-3′	71 bp	NM_009447

structure, a single experiment was performed over two days protocol. Brain slices (three *per* animal) were selected at different Bregma (B) (dHPC from B = −1.34 mm until B = −2.46 mm; vHPC from B = −2.92 mm until B = −3.64 mm). Fluorescein (FITC, for CB1) and Digoxigenin (DIG, for GAD65/67)-labeled riboprobes were used. The antisense probes were hybridized to their cellular mRNA counterpart, sense probes were included to control the specificity of the hybridization. To avoid RNA degradation, all solutions were treated with active diethyl pyrocarbonate (DEPC), a RNases inhibitor. The hybridization was conducted over night at 60 °C and post-hybridization washes at 65 °C were essential to fix the probes. The probes were detected one after the other using antibody-peroxidase POD conjugates (Roche) specific for DIG and Fluorescein. In order to maintain specificity, a quenching step after the first POD-conjugate inhibited the POD enzyme presented with the first antibody. The antibody bound POD triggered the accumulation of the tyramide signal amplification (TSA)-coupled with the fluorescent stain Cyanine 3-labeled tyramide (Perkin Elmer; 1:100 for 10 min) to label GAD65/67 signal and FITC-conjugated tyramide (Perkin Elmer; 1:80 for 12 min) to detect the *Cnr1* mRNA. Later, incubation with 4′,6-diamidino-2-phenylindole (DAPI; 1:20000; FISHER Scientific) was performed for 5 min to detect the cell nucleus. After the final washings, slices were coverslipped and signals were assessed in epifluorescence Leica DM6000 microscope. Reagents are summarized in Table 2.

4.9. Image quantification

The number of cells and the intensity of signal were evaluated for CB1-positive cells, GAD65/67 positive cells and CB1 in GAD65/67-positive cells within different regions of dHPC and vHPC. In the hippocampi, analyses were performed in fixed areas as described in Figs. 5 and 6, within the pyramidal layer (*Py*) and radiatum and lacunosum moleculare strata (*LMol*) (threshold 4.95% and 1% respectively) in *CA1*; pyramidal layer (*Py*) and stratum lucidum (*SLu*) (threshold 4.95% and 2,95% respectively) in *CA3*; granular dentate gyrus (*DG-Gr*) and polymorph dentate gyrus (*DG-Po*) (threshold 6.51% and 2.95% respectively) for *DG*. Quantifications were performed on 10× magnification images (100 μm scale) taken with a LEICA DM600 epifluorescence microscope. For quantification, Image J software (NIH, USA; ImageJ (RRID:SCR_003070) was used and a calculated permanent threshold (thr) was applied from the corresponding region of CB1-KO as negative control for CB1 (for *Py* thr = 4.95%, for *LMol* thr = 1%, for *SLu* and *Po-DG* thr = 2.95%, for *Gr-DG* thr = 6.51%). A fixed area was reproduced in each image and the quantification was performed with image J and confirmed manually.

Table 2
Reagent, source and batch for *in situ* hybridization.

Reagent	Source	Batch
Anti-Digoxigenin-Horseradish peroxidase (HRP)	Sigma-Aldrich	CAT#11207733910; RRID: AB_514500
Anti-Fluorescein-POD-Horseradish peroxidase (HRP)	Sigma-Aldrich	CAT#11426346910; RRID: AB_840257
Donkey Anti-Goat Alexa 488	Fischer Scientific	CAT#A-11055; RRID: AB_2534102
DIG riboprobes against GAD65/67	(Marsicano and Lutz, 1999)	Riboprobes GAD65-DIG lab stock
FITC riboprobes against CB1	(Marsicano and Lutz, 1999)	Riboprobes CB1-FITC lab stock
Gold-labeled rabbit anti-goat Immunoglobulin G	Nanoprobes	CAT#2004; RRID: AB_2631182
Cyanine 3-labeled tyramide (TSA)	Perkin Elmer	CAT#NEL744001KT
FITC-conjugated tyramide (TSA)	Perkin Elmer	CAT#NEL741001KT

4.10. Statistics

All experiments involving mice were performed according to the protocols approved by the Aquitaine-Poitou Charentes local ethics committee (authorization number APAFIS#26733-2020072417531214 v2) in strict compliance with the French Ministry of Agriculture and Fisheries (authorization number D33-063-096) and European Union Council Directive (2010/63/EU). All efforts were made to minimize animal suffering and to reduce the number of mice used, while maintaining reliable statistics. All experiments were conducted with experimenters blind to genotype; no randomization method for the constitution of the experimental groups was applied. The sample size was chosen to ensure adequate statistical power for all experiments. All values were given as mean ± s.e.m. and the statistical analysis were performed using GraphPad Prism 7 software (GraphPad Software Inc., San Diego, USA). The normality of the data distribution was verified using the Shapiro-Wilk normality test. Depending the assumptions of normality, the non-parametric two-tailed Mann-Whitney test or the parametric unpaired *t*-test was used. Statistical significance was expressed as $*p < 0.05$; $**p < 0.01$; $***p < 0.001$.

Supplementary data to this article can be found online at https://doi.org/10.1016/j.mcn.2022.103705.

CRediT authorship contribution statement

Conceptualization: JM.R, M.V; Methodology: N.DF, G.D, A.G, V.RL, V.L, F.JK, T.LL, A.C, I.M, D.G; Data analysis: JM.R, M.V, G.D, N.DF, D.C, V.S, G.M, PV.P; Resources: JM.R; Writing: JM.R, M.V, D.C, G.M; Supervision: JM.R, M.V; Project administration: JM.R; Funding acquisition: JM.R.

Declaration of competing interest

The authors declare no competing interests.

Acknowledgements

Supported by CNRS (JM.R, M.V.) INSERM (V. RL, F.JK, V.L, A.G., T. LL, I.M, A.C, D.G, D.C, G.M, PV.P) and University of Bordeaux (G.D). This work benefited from the support of the Animal Breeding and Housing (Sara Laumond), and the Genotyping (Delphine Gonzales), Analytical chemistry (Isabelle Matias), Transcriptomic (Thierry Leste-Lasserre) and bioinformatics (Alexandre Brochard) facilities of the Magendie Neurocentre funded by the Inserm and LABEX BRAIN (ANR-10-LABX-43). The 'Biochemistry and Biophysics Facility' of the Bordeaux Neurocampus was funded by LABEX BRAIN (ANR-10-LABX-43). N.DF was funded by a grant from the Aquitaine Regional Council and INSERM. V.S was funded by a grant from LABEX BRAIN to D.C.

Funding

This work was financially supported by INSERM (U1215SE19GA and RVF14001GGA), Aquitaine Regional Council, and University of Bordeaux.

References

Abrous, D.N., Koehl, M., Le Moal, M., 2005. Adult neurogenesis: from precursors to network and physiology. Physiol. Rev. 85 (2), 523–569. https://doi.org/10.1152/physrev.00055.2003.

Ahmed, Md.M., et al., 2012. Loss of correlations among proteins in brains of the Ts65Dn mouse model of down syndrome. J. Proteome Res. 11 (2), 1251–1263. https://doi.org/10.1021/pr2011582.

Ahn, H.J., et al., 2008. c-Rel, an NF-κB family transcription factor, is required for hippocampal long-term synaptic plasticity and memory formation. Learn. Mem. 15 (7), 539–549. https://doi.org/10.1101/lm.866408.

Alemany-González, M., et al., 2020. Prefrontal–hippocampal functional connectivity encodes recognition memory and is impaired in intellectual disability. Proc. Natl. Acad. Sci. 117 (21), 11788–11798. https://doi.org/10.1073/pnas.1921314117.

Altafaj, X., et al., 2001. Neurodevelopmental delay, motor abnormalities and cognitive deficits in transgenic mice overexpressing Dyrk1A (minibrain), a murine model of Down's syndrome. Hum. Mol. Genet. 10 (18), 1915–1923. https://doi.org/10.1093/hmg/10.18.1915.

Altamura, C., et al., 2015. Elevation of plasma 2-arachidonoylglycerol levels in Alzheimer's disease patients as a potential protective mechanism against neurodegenerative decline. J. Alzheimers Dis. 46 (2), 497–506. https://doi.org/10.3233/JAD-142349.

Antonarakis, S.E., 2017. Down syndrome and the complexity of genome dosage imbalance. Nat. Rev. Genet. 18 (3), 147–163. https://doi.org/10.1038/nrg.2016.154.

Aylward, E.H., et al., 1999. MRI volumes of the hippocampus and amygdala in adults with Down's syndrome with and without dementia. Am. J. Psychiatry 5.

Aziz, N.M., et al., 2018. Lifespan analysis of brain development, gene expression and behavioral phenotypes in the Ts1Cje, Ts65Dn and Dp(16)1/Yey mouse models of Down syndrome. Dis. Model. Mech. 11 (6) https://doi.org/10.1242/dmm.031013.

Basavarajappa, B.S., 2007. Critical enzymes involved in endocannabinoid metabolism. Protein Peptide Lett. 14 (3), 237–246.

Belichenko, P.V., et al., 2007. Synaptic and cognitive abnormalities in mouse models of down syndrome: exploring genotype-phenotype relationships. J. Comp. Neurol. 504 (4), 329–345. https://doi.org/10.1002/cne.21433.

Belichenko, P.V., et al., 2015. Down syndrome cognitive phenotypes modeled in mice trisomic for All HSA 21 homologues. In: Herault, Y. (Ed.), PLOS ONE, 10(7). https://doi.org/10.1371/journal.pone.0134861 p. e0134861.

Bilsland, L.G., et al., 2006. Increasing cannabinoid levels by pharmacological and genetic manipulation delay disease progression in SOD1 mice. FASEB J. 20 (7), 1003–1005. https://doi.org/10.1096/fj.05-4743fje.

Bouarab, C., et al., 2021. PAI-1 protein is a key molecular effector in the transition from normal to PTSD-like fear memory. Mol. Psychiatry 26 (9), 4968–4981. https://doi.org/10.1038/s41380-021-01024-1.

Busquets-Garcia, A., et al., 2015. Dissecting the cannabinergic control of behavior: the where matters. BioEssays 37 (11), 1215–1225. https://doi.org/10.1002/bies.201500046.

Busquets-Garcia, A., et al., 2017. Pregnenolone blocks cannabinoid-induced acute psychotic-like states in mice. Mol. Psychiatry 22 (11), 1594–1603. https://doi.org/10.1038/mp.2017.4.

Busquets-Garcia, A., Bains, J., Marsicano, G., 2018. CB1 receptor signaling in the brain: extracting specificity from ubiquity. Neuropsychopharmacology 43 (1), 4–20. https://doi.org/10.1038/npp.2017.206.

Bustin, S.A., et al., 2009. The MIQE guidelines: minimum information for publication of quantitative real-time PCR experiments. Clin. Chem. 55 (4), 611–622. https://doi.org/10.1373/clinchem.2008.112797.

Caban-Holt, A., Head, E., Schmitt, F., 2015. Chapter 15 - down syndrome. In: Rosenberg, R.N., Pascual, J.M. (Eds.), Rosenberg's Molecular And Genetic Basis of Neurological And Psychiatric Disease, Fifth edition. Academic Press, Boston, pp. 163–170. https://doi.org/10.1016/B978-0-12-410529-4.00015-2.

Chakrabarti, L., et al., 2010. Olig1 and Olig2 triplication causes developmental brain defects in Down syndrome. Nat. Neurosci. 13 (8), 927–934. https://doi.org/10.1038/nn.2600.

Chao, O.Y., et al., 2020. The medial prefrontal cortex - hippocampus circuit that integrates information of object, place and time to construct episodic memory in rodents: behavioral, anatomical and neurochemical properties. Neurosci. Biobehav. Rev. 113, 373–407. https://doi.org/10.1016/j.neubiorev.2020.04.007.

Chomczynski, P., Sacchi, N., 1987. Single-step method of RNA isolation by acid guanidinium thiocyanate-phenol-chloroform extraction. Anal. Biochem. 162 (1), 156–159. https://doi.org/10.1006/abio.1987.9999.

Christensen, R., et al., 2007. Efficacy and safety of the weight-loss drug rimonabant: a meta-analysis of randomised trials. Lancet (London, England) 370 (9600), 1706–1713. https://doi.org/10.1016/S0140-6736(07)61721-8.

Cota, D., 2007. CB1 receptors: emerging evidence for central and peripheral mechanisms that regulate energy balance, metabolism, and cardiovascular health. Diabetes Metab. Res. Rev. 23 (7), 507–517. https://doi.org/10.1002/dmrr.764.

Davisson, M.T., Schmidt, C., Akeson, E.C., 1990. Segmental trisomy of murine chromosome 16: a new model system for studying Down syndrome. Prog. Clin. Biol. Res. 360, 263–280.

Davisson, M.T., et al., 1993. Segmental trisomy as a mouse model for Down syndrome. Prog. Clin. Biol. Res. 384, 117–133.

DeLong, G., et al., 2010. Pharmacological evaluation of the natural constituent of Cannabis sativa, cannabichromene and its modulation by Δ(9)-tetrahydrocannabinol. Drug Alcohol Depend. 112, 126–133. https://doi.org/10.1016/j.drugalcdep.2010.05.019.

Dierssen, M., 2012. Down syndrome: the brain in trisomic mode. Nat. Rev. Neurosci. 13 (12), 844–858. https://doi.org/10.1038/nrn3314.

Duchon, A., et al., 2011. Identification of the translocation breakpoints in the Ts65Dn and Ts1Cje mouse lines: relevance for modeling Down syndrome. Mamm. Genome 22 (11), 674–684. https://doi.org/10.1007/s00335-011-9356-0.

Duchon, A., et al., 2021. Multi-influential genetic interactions alter behaviour and cognition through six main biological cascades in Down syndrome mouse models. Hum. Mol. Genet. 30 (9), 771–788. https://doi.org/10.1093/hmg/ddab012.

Escorihuela, R.M., et al., 1998. Impaired short- and long-term memory in Ts65Dn mice, a model for Down syndrome. Neurosci. Lett. 247 (2–3), 171–174. https://doi.org/10.1016/S0304-3940(98)00317-6.

Fanselow, M.S., Dong, H.-W., 2010. Are the dorsal and ventral hippocampus functionally distinct structures? Neuron 65 (1), 7–19. https://doi.org/10.1016/j.neuron.2009.11.031.

Ferbinteanu, J., McDonald, R.J., 2001. Dorsal/ventral hippocampus, fornix, and conditioned place preference. Hippocampus 11 (2), 187–200. https://doi.org/10.1002/hipo.1036.

Fong, T.M., 2014. Constitutive activity in cannabinoid receptors. Adv. Pharmacol. (San Diego, Calif.) 70, 121–133. https://doi.org/10.1016/B978-0-12-417197-8.00004-3.

Gardiner, K.J., 2015. Pharmacological approaches to improving cognitive function in down syndrome: current status and considerations. Drug Des. Dev. Ther. 9, 103–125. https://doi.org/10.2147/DDDT.S51476.

Gardiner, K., et al., 2010. Down syndrome: from understanding the neurobiology to therapy. J. Neurosci. 30 (45), 14943–14945. https://doi.org/10.1523/JNEUROSCI.3728-10.2010.

Gupta, M., Dhanasekaran, A.R., Gardiner, K.J., 2016. Mouse models of down syndrome: gene content and consequences. Mamm. Genome 27 (11–12), 538–555. https://doi.org/10.1007/s00335-016-9661-8.

Han, J., et al., 2012. Acute cannabinoids impair working memory through astroglial CB1 receptor modulation of hippocampal LTD. Cell 148 (5), 1039–1050. https://doi.org/10.1016/j.cell.2012.01.037.

Hebert-Chatelain, E., et al., 2016. A cannabinoid link between mitochondria and memory. Nature 539 (7630), 555–559. https://doi.org/10.1038/nature20127.

Helguera, P., et al., 2013. Adaptive downregulation of mitochondrial function in down syndrome. Cell Metab. 17 (1), 132–140. https://doi.org/10.1016/j.cmet.2012.12.005.

Henke, P.G., 1990. Hippocampal pathway to the amygdala and stress ulcer development. Brain Res. Bull. 25 (5), 691–695. https://doi.org/10.1016/0361-9230(90)90044-Z.

Herault, Y., et al., 2017. Rodent models in Down syndrome research: impact and future opportunities. Dis. Model. Mech. 10 (10), 1165–1186. https://doi.org/10.1242/dmm.029728.

Hernández-González, S., et al., 2014. Altered distribution of hippocampal interneurons in the murine Down syndrome model Ts65Dn. Neurochem. Res. 40 https://doi.org/10.1007/s11064-014-1479-8.

Hobson-Rohrer, W.L., Samson-Fang, L., 2013. Down syndrome. Pediatr. Rev. 34 (12), 573–574. https://doi.org/10.1542/pir.34-12-573.

Houser, C.R., Esclapez, M., 1994. Localization of mRNAs encoding two forms of glutamic acid decarboxylase in the rat hippocampal formation. Hippocampus 4 (5), 530–545. https://doi.org/10.1002/hipo.450040503.

Hunter, C.L., Bachman, D., Granholm, A.-C., 2004. Minocycline prevents cholinergic loss in a mouse model of Down's syndrome. Ann. Neurol. 56 (5), 675–688. https://doi.org/10.1002/ana.20250.

Hyde, L.A., et al., 2001. Motor learning in Ts65Dn mice, a model for Down syndrome. Dev. Psychobiol. 38 (1), 33–45. https://doi.org/10.1002/1098-2302(2001)38:1<33::aid-dev3>3.0.co;2-0.
Insausti, R., et al., 1998. Human medial temporal lobe in aging: anatomical basis of memory preservation. Microsc. Res. Tech. 43 (1), 8–15. https://doi.org/10.1002/(SICI)1097-0029(19981001)43:1<8::AID-JEMT2>3.0.CO;2-4.
Jacob, W., et al., 2012. Cannabinoid CB1 receptor deficiency increases contextual fear memory under highly aversive conditions and long-term potentiation in vivo. Neurobiol. Learn. Mem. 98 (1), 47–55. https://doi.org/10.1016/j.nlm.2012.04.008.
Jordan, C.J., Xi, Z.-X., 2019. Progress in brain cannabinoid CB2 receptor research: from genes to behavior. Neurosci. Biobehav. Rev. 98, 208–220. https://doi.org/10.1016/j.neubiorev.2018.12.026.
Kano, M., et al., 2009. Endocannabinoid-mediated control of synaptic transmission. Physiol. Rev. 89 (1), 309–380. https://doi.org/10.1152/physrev.00019.2008.
Katona, I., Freund, T.F., 2012. Multiple functions of endocannabinoid signaling in the brain. Annu. Rev. Neurosci. 35, 529–558. https://doi.org/10.1146/annurev-neuro-062111-150420.
Kawamura, Y., et al., 2006. The CB1 cannabinoid receptor is the major cannabinoid receptor at excitatory presynaptic sites in the hippocampus and cerebellum. J. Neurosci. 26 (11), 2991–3001. https://doi.org/10.1523/JNEUROSCI.4872-05.2006.
Kim, S.R., et al., 2005. Transient receptor potential vanilloid subtype 1 mediates cell death of mesencephalic dopaminergic neurons in vivo and in vitro. J. Neurosci. 25 (3), 662–671. https://doi.org/10.1523/JNEUROSCI.4166-04.2005.
Kjelstrup, K.G., et al., 2002. Reduced fear expression after lesions of the ventral hippocampus. Proc. Natl. Acad. Sci. 99 (16), 10825–10830. https://doi.org/10.1073/pnas.152112399.
Kleschevnikov, A.M., et al., 2004. Hippocampal long-term potentiation suppressed by increased inhibition in the Ts65Dn mouse, a genetic model of Down syndrome. J. Neurosci. 24 (37), 8153–8160. https://doi.org/10.1523/JNEUROSCI.1766-04.2004.
Kurt, M.A., et al., 2004. Deficits of neuronal density in CA1 and synaptic density in the dentate gyrus, CA3 and CA1, in a mouse model of Down syndrome. Brain Res. 1022 (1–2), 101–109. https://doi.org/10.1016/j.brainres.2004.06.075.
Lana-Elola, E., et al., 2011. Down syndrome: searching for the genetic culprits. Dis. Model. Mech. 4 (5), 586–595. https://doi.org/10.1242/dmm.008078.
Laprairie, R.B., Kelly, M.E.M., Denovan-Wright, E.M., 2012. The dynamic nature of type 1 cannabinoid receptor (CB(1)) gene transcription. Br. J. Pharmacol. 167 (8), 1583–1595. https://doi.org/10.1111/j.1476-5381.2012.02175.x.
Li, Z., et al., 2007. Duplication of the entire 22.9 Mb human chromosome 21 syntenic region on mouse chromosome 16 causes cardiovascular and gastrointestinal abnormalities. Hum. Mol. Genet. 16 (11), 1359–1366. https://doi.org/10.1093/hmg/ddm086.
Livak, K.J., Schmittgen, T.D., 2001. Analysis of relative gene expression data using real-time quantitative PCR and the 2(-Delta Delta C(T)) Method. Methods 25 (4), 402–408. https://doi.org/10.1006/meth.2001.1262.
Lorenzi, H.A., Reeves, R.H., 2006. Hippocampal hypocellularity in the Ts65Dn mouse originates early in development. Brain Res. 1104 (1), 153–159. https://doi.org/10.1016/j.brainres.2006.05.022.
Lott, I.T., 2012. Antioxidants in Down syndrome. Biochim. Biophys. Acta 1822 (5), 657–663. https://doi.org/10.1016/j.bbadis.2011.12.010.
Lu, H.-C., Mackie, K., 2016. An introduction to the endogenous cannabinoid system. Biol. Psychiatry 79 (7), 516–525. https://doi.org/10.1016/j.biopsych.2015.07.028.
Lysenko, L.V., et al., 2014. Monoacylglycerol lipase inhibitor JZL184 improves behavior and neural properties in Ts65Dn mice, a model of Down syndrome. In: Yan, R. (Ed.), PLoS ONE, 9(12). https://doi.org/10.1371/journal.pone.0114521 p. e114521.
Maccarrone, M., Battista, N., Centonze, D., 2007. The endocannabinoid pathway in Huntington's disease: a comparison with other neurodegenerative diseases. Prog. Neurobiol. 81 (5–6), 349–379. https://doi.org/10.1016/j.pneurobio.2006.11.006.
Marsicano, G., Lafenêtre, P., 2009. Roles of the endocannabinoid system in learning and memory. Curr. Top. Behav. Neurosci. 1, 201–230. https://doi.org/10.1007/978-3-540-88955-7_8.
Marsicano, G., Lutz, B., 1999. Expression of the cannabinoid receptor CB1 in distinct neuronal subpopulations in the adult mouse forebrain: CB1 expression in murine forebrain. Eur. J. Neurosci. 11 (12), 4213–4225. https://doi.org/10.1046/j.1460-9568.1999.00847.x.
Marsicano, G., et al., 2002. The endogenous cannabinoid system controls extinction of aversive memories. Nature 418 (6897), 530–534. https://doi.org/10.1038/nature00839.
Martin, S.J., Clark, R.E., 2007. The rodent hippocampus and spatial memory: from synapses to systems. Cell. Mol. Life Sci. 64 (4), 401–431. https://doi.org/10.1007/s00018-007-6336-3.
Martínez-Cué, C., et al., 2002. Differential effects of environmental enrichment on behavior and learning of male and female Ts65Dn mice, a model for down syndrome. Behav. Brain Res. 134 (1–2), 185–200. https://doi.org/10.1016/s0166-4328(02)00026-8.
Matias, I., et al., 2012. Endocannabinoids measurement in human saliva as potential biomarker of obesity. PloS One 7 (7), e42399. https://doi.org/10.1371/journal.pone.0042399.
Mojabi, F.S., et al., 2016. GABAergic hyperinnervation of dentate granule cells in the Ts65Dn mouse model of Down syndrome: exploring the role of app: GABAergic interneurons in down syndrome. Hippocampus 26 (12), 1641–1654. https://doi.org/10.1002/hipo.22664.
Moser, M.B., Moser, E.I., 1998. Functional differentiation in the hippocampus. Hippocampus 8 (6), 608–619. https://doi.org/10.1002/(SICI)1098-1063(1998)8:6<608::AID-HIPO3>3.0.CO;2-7.
Moser, M.B., et al., 1995. Spatial learning with a minislab in the dorsal hippocampus. Proc. Natl. Acad. Sci. 92 (21), 9697–9701. https://doi.org/10.1073/pnas.92.21.9697.
Navarro-Romero, A., et al., 2019. Cannabinoid type-1 receptor blockade restores neurological phenotypes in two models for Down syndrome. Neurobiol. Dis. 125, 92–106. https://doi.org/10.1016/j.nbd.2019.01.014.
Perluigi, M., Butterfield, D.A., 2012. Oxidative stress and Down syndrome: a route toward Alzheimer-like dementia. Curr. Gerontol. Geriatr. Res. 2012 https://doi.org/10.1155/2012/724904.
Pothuizen, H.H.J., et al., 2004. Dissociation of function between the dorsal and the ventral hippocampus in spatial learning abilities of the rat: a within-subject, within-task comparison of reference and working spatial memory. Eur. J. Neurosci. 19 (3), 705–712. https://doi.org/10.1111/j.0953-816X.2004.03170.x.
Preston, A.R., Eichenbaum, H., 2013. Interplay of hippocampus and prefrontal cortex in memory. Curr. Biol. 23 (17), R764–R773. https://doi.org/10.1016/j.cub.2013.05.041.
Puighermanal, E., et al., 2012. Cellular and intracellular mechanisms involved in the cognitive impairment of cannabinoids. Philos. Trans. R. Soc. B: Biol. Sci. 367 (1607), 3254–3263. https://doi.org/10.1098/rstb.2011.0384.
Ramirez, B.G., 2005. Prevention of Alzheimer's disease pathology by cannabinoids: neuroprotection mediated by blockade of microglial activation. J. Neurosci. 25 (8), 1904–1913. https://doi.org/10.1523/JNEUROSCI.4540-04.2005.
Reeves, R.H., et al., 1995. A mouse model for Down syndrome exhibits learning and behaviour deficits. Nat. Genet. 11 (2), 177–184. https://doi.org/10.1038/ng1095-177.
Rice, J., Cameron, M., 2018. Cannabinoids for treatment of MS symptoms: state of the evidence. Curr. Neurol. Neurosci. Rep. 18 (8), 50. https://doi.org/10.1007/s11910-018-0859-x.
Riedel, G., Davies, S.N., 2005. Cannabinoid function in learning,memory and plasticity. Cannabinoids 445–477. https://doi.org/10.1007/3-540-26573-2_15.
Rowe, J., Lavender, A., Turk, V., 2006. Cognitive executive function in Down's syndrome. Br. J. Clin. Psychol. 45 (Pt 1), 5–17. https://doi.org/10.1348/014466505X29594.
Seely, K.A., et al., 2012. AM-251 and rimonabant act as direct antagonists at mu-opioid receptors: implications for opioid/cannabinoid interaction studies. Neuropharmacology 63 (5), 905–915. https://doi.org/10.1016/j.neuropharm.2012.06.046.
Silva-Cruz, A., et al., 2017. Dual influence of endocannabinoids on long-term potentiation of synaptic transmission. Front. Pharmacol. 8 https://doi.org/10.3389/fphar.2017.00921.
Souchet, B., et al., 2015. Pharmacological correction of excitation/inhibition imbalance in Down syndrome mouse models. Front. Behav. Neurosci. 9 https://doi.org/10.3389/fnbeh.2015.00267.
Sturgeon, X., et al., 2012. Pathways to cognitive deficits in Down syndrome. Prog. Brain Res. 197, 73–100. https://doi.org/10.1016/B978-0-444-54299-1.00005-4.
Sugiura, T., 2008. Biosynthesis of anandamide and 2-arachidonoylglycerol. In: Cannabinoids And the Brain, pp. 15–30. https://doi.org/10.1007/978-0-387-74349-3_2.
Teipel, S.J., et al., 2003. Relation of corpus callosum and hippocampal size to age in nondemented adults with Down's syndrome. Am. J. Psychiatry 160 (10), 1870–1878. https://doi.org/10.1176/appi.ajp.160.10.1870.
Terral, G., et al., 2019. CB1 receptors in the anterior piriform cortex control odor preference memory. Curr. Biol. 29 (15), 2455–2464.e5. https://doi.org/10.1016/j.cub.2019.06.041.
Toma, I.D., Sierra, C., Dierssen, M., 2021. Meta-analysis of transcriptomic data reveals clusters of consistently deregulated gene and disease ontologies in Down syndrome. PLoS Comput. Biol. 17 (9), e1009317 https://doi.org/10.1371/journal.pcbi.1009317.
Vallée, M., et al., 2014. Pregnenolone can protect the brain from cannabis intoxication. Science 343 (6166), 94–98. https://doi.org/10.1126/science.1243985.
Vandesompele, J., et al., 2002. Accurate normalization of real-time quantitative RT-PCR data by geometric averaging of multiple internal control genes. Genome Biol. 3 (7) https://doi.org/10.1186/gb-2002-3-7-research0034 p. research0034.1.
Vázquez-Oliver, A., et al., 2021. Long-term decreased cannabinoid type-1 receptor activity restores specific neurological phenotypes in the Ts65Dn mouse model of Down syndrome. Neuroscience. https://doi.org/10.1101/2021.11.22.469296. Preprint.
Vis, J.C., et al., 2009. Down syndrome: a cardiovascular perspective. J. Intellect. Disab. Res. 53 (5), 419–425. https://doi.org/10.1111/j.1365-2788.2009.01158.x.
Yu, T., et al., 2010. Effects of individual segmental trisomies of human chromosome 21 syntenic regions on hippocampal long-term potentiation and cognitive behaviors in mice. Brain Res. 1366, 162–171. https://doi.org/10.1016/j.brainres.2010.09.107.
Zanettini, C., 2011. Effects of endocannabinoid system modulation on cognitive and emotional behavior. Front. Behav. Neurosci. 5 https://doi.org/10.3389/fnbeh.2011.00057.